

The SGWB produced by MHD turbulence in the early universe

Progress on Old and New Themes in Cosmology (PONT)

May 2, 2023
Avignon, France

Alberto Roper Pol
SNSF Ambizione fellow
University of Geneva



Collaborators: A. Brandenburg (Nordita), C. Caprini (UniGe & CERN), T. Kahniashvili (CMU), A. Kosowsky (PittU), S. Mandal (SBU), A. Midiri (UniGe), A. Neronov (APC), D. Semikoz (APC)

ARP *et al.*, *Geophys. Astrophys. Fluid Dyn.* **114**, 130 (2020), arXiv:1807.05479

ARP *et al.*, *Phys. Rev. D* **102**, 083512 (2020), arXiv:1903.08585

ARP *et al.*, *JCAP* **04** (2022), 019, arXiv:2107.05356

ARP, C. Caprini, A. Neronov, D. Semikoz, *Phys. Rev. D* **105**, 123502 (2022), arXiv:2201.05630.

https://github.com/AlbertoRoper/GW_turbulence

Probing the early Universe with GWs

Cosmological (pre-recombination) GW background

- Why background? Individual sources are not resolvable, superposition of single events occurring in the whole Universe.
- Phase transitions
 - Ground-based detectors (LVK, ET, CE) frequencies are 10–1000 Hz
Peccei-Quinn, B-L, left-right symmetries, ... $\sim 10^7, 10^8$ GeV
(untested physics).
 - Space-based detectors (**LISA**) frequencies are 10^{-5} – 10^{-2} Hz
Electroweak phase transition ~ 100 GeV
 - Pulsar Timing Array (**PTA**) frequencies are 10^{-9} – 10^{-7} Hz
Quark confinement (QCD) phase transition ~ 100 MeV
- From inflation
 - B -modes of CMB anisotropies ($f_c \sim 10^{-18}$ Hz).
 - Can cover all f spectrum, depending on end-of-reheating T , and blue-tilted (beyond slow-roll inflation).

Cosmological GWs

Cosmological GWs have the potential to provide us with *direct information on early universe physics* that is *not accessible via electromagnetic observations, possibly complementary to collider experiments*:

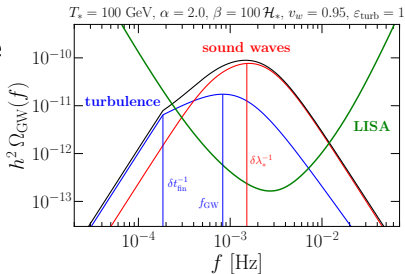
nature of first-order phase transitions (baryogenesis, BSM physics, high-energy physics), **origin of primordial magnetic fields**.

MHD sources in the early universe

- Magnetohydrodynamic (MHD) sources of GWs:
 - Sound waves generated from first-order phase transitions.
 - (M)HD turbulence from first-order phase transitions.
 - **Primordial magnetic fields.**
- High-conductivity of the early universe leads to a high-coupling between magnetic and velocity fields.

- Other sources of GWs include

- Bubble collisions.
- Cosmic strings.
- Primordial black holes.
- Inflation.



Primordial magnetic fields

- Magnetic fields can either be produced at or present during cosmological phase transitions.
- The magnetic fields are strongly coupled to the primordial plasma and inevitably lead to MHD turbulence.¹
- Present magnetic fields can be amplified by primordial turbulence via dynamo.²
- Primordial magnetic fields would evolve through the history of the universe up to the present time and could explain the lower bounds in cosmic voids derived by the Fermi collaboration.³
- Maximum amplitude of primordial magnetic fields is constrained by the big bang nucleosynthesis.⁴
- Additional constraints from CMB, Faraday Rotation, ultra-high energy cosmic rays (UHECR).

¹ J. Ahonen and K. Enqvist, *Phys. Lett. B* **382**, 40 (1996).

² A. Brandenburg *et al.* (incl. ARP), *Phys. Rev. Fluids* **4**, 024608 (2019).

³ A. Neronov and I. Vovk, *Science* **328**, 73 (2010).

⁴ V. F. Shvartsman, *Pisma Zh. Eksp. Teor. Fiz.* **9**, 315 (1969).

Generation of primordial magnetic fields

- Bubble collisions and velocity fields induced by first-order phase transitions can generate magnetic fields.
- Parity-violating processes during the EWPT are predicted by SM extensions that account for baryogenesis and can produce helical magnetic fields.⁵
- Axion fields can amplify and produce magnetic field helicity.⁶
- Magnetic fields from inflation can be present during phase transitions (non-helical⁷ and helical⁸).
- Low-scale (QCD and EWPT) inflationary magnetogenesis.⁹
- Chiral magnetic effect.¹⁰

⁵T. Vachaspati, *Phys. Rev. B* **265**, 258 (1991), T. Vachaspati, *Phys. Rev. Lett.* **87**, 251302 (2001), J. M. Cornwall, *Phys. Rev. D* **56**, 6146 (1997).

⁶M. M. Forbes and A. R. Zhitnitsky, *Phys. Rev. Lett.* **85**, 5268 (2000).

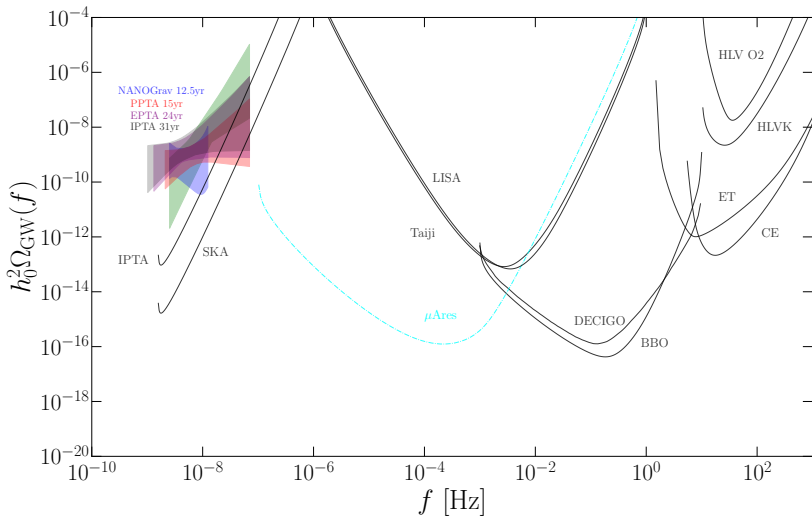
⁷M. S. Turner and L. M. Widrow, *Phys. Rev. D* **37**, 2743 (1988).

⁸M. Giovannini, *Phys. Rev. D* **58**, 124027 (1998).

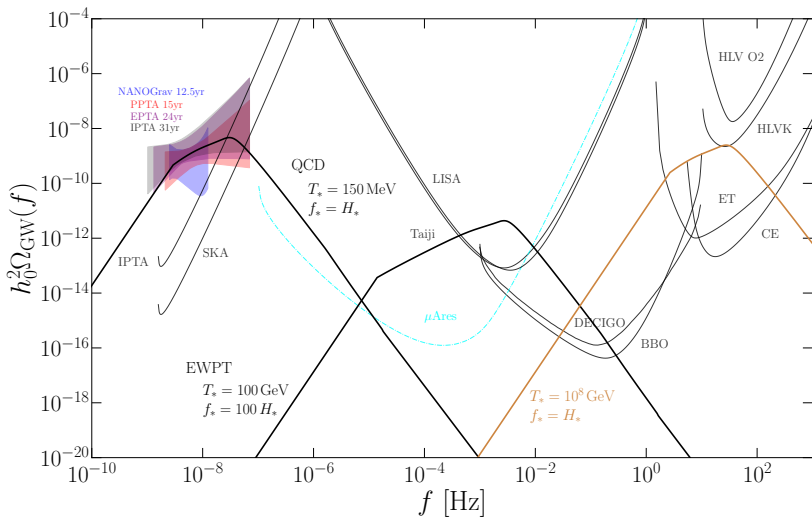
⁹R. Sharma, *Phys. Rev. D* **97**, 083503 (2018).

¹⁰M. Joyce and M. E. Shaposhnikov, *PRL* **79**, 1193 (1997).

Gravitational wave detectors



Gravitational spectrum (turbulence from PTs)¹¹




¹¹ ARP, C. Caprini, A. Neronov, D. Semikoz, *PRD* **105**, 123502 (2022)

A. Neronov, ARP, C. Caprini, D. Semikoz, *PRD* **103**, L041302 (2021).

How do we compute these signals?

- Direct numerical simulations using the PENCIL CODE¹² to solve:
 - ① Relativistic MHD equations adapted for radiation-dominated era (after electroweak symmetry is broken).
 - ② Gravitational waves equation.
- Numerical simulations are *in general* necessary to solve MHD dynamics and to take into account the exact unequal time correlator of the GW sourcing term (analytical estimates require simplifying assumptions).

¹²Pencil Code Collaboration, JOSS 6, 2807 (2020), <https://github.com/pencil-code/> 

MHD description

Right after the electroweak phase transition we can model the plasma using continuum MHD.

- Charge-neutral, electrically conducting fluid.
- Relativistic magnetohydrodynamic (MHD) equations.
- Radiation-dominated Universe

$$p = \rho c^2/3,$$

i.e. $w = 1/3$ (ultrarelativistic EoS).

- Friedmann–Lemaître–Robertson–Walker metric

$$g_{\mu\nu} = \text{diag}\{-1, a^2, a^2, a^2\}$$

Contributions to the stress-energy tensor

$$T^{\mu\nu} = (\rho/c^2 + \rho) U^\mu U^\nu + p g^{\mu\nu} + \pi^{\mu\nu} + F^{\mu\gamma} F^\nu{}_\gamma - \frac{1}{4} g^{\mu\nu} F_{\lambda\gamma} F^{\lambda\gamma}$$

- From fluid motions:

$$T_{ij} = (\rho/c^2 + \rho) \gamma^2 u_i u_j + p \delta_{ij}$$

- Ultrarelativistic EoS:

$$p = \rho c^2 / 3$$

- Viscous stresses: $\pi_{ij} =$

$$\nu(\rho/c^2 + \rho)(u_{i,j} + u_{j,i})$$

- 4-velocity $U^\mu = \gamma(c, u^i)$
- 4-potential $A^\mu = (\phi/c, A^i)$

- From magnetic fields:

$$T_{ij} = -B_i B_j + \delta_{ij} B^2 / 2$$

- 4-current $J^\mu = (c\rho_e, J^i)$

- Faraday tensor

$$F_{\mu\nu} = \partial_\mu A_\nu - \partial_\nu A_\mu$$

Conservation laws

$$T^{\mu\nu}{}_{;\nu} = 0$$

We assume subrelativistic motions:

$$\gamma^2 \sim 1 + (v/c)^2 + \mathcal{O}(v/c)^4$$

Relativistic MHD equations are reduced to¹³

$$\frac{\partial \ln \rho}{\partial t} = -\frac{4}{3} (\nabla \cdot \mathbf{u} + \mathbf{u} \cdot \nabla \ln \rho) + \frac{1}{\rho} [\mathbf{u} \cdot (\mathbf{J} \times \mathbf{B}) + \eta J^2],$$

$$\begin{aligned} \frac{D\mathbf{u}}{Dt} &= \frac{1}{3} \mathbf{u} (\nabla \cdot \mathbf{u} + \mathbf{u} \cdot \nabla \ln \rho) - \frac{\mathbf{u}}{\rho} [\mathbf{u} \cdot (\mathbf{J} \times \mathbf{B}) + \eta J^2] \\ &\quad - \frac{1}{4} \nabla \ln \rho + \frac{3}{4\rho} \mathbf{J} \times \mathbf{B} + \frac{2}{\rho} \nabla \cdot (\rho \nu \mathbf{S}) + \mathcal{F}, \end{aligned}$$

$$\frac{\partial \mathbf{B}}{\partial t} = \nabla \times (\mathbf{u} \times \mathbf{B} - \eta \mathbf{J} + \mathcal{E}), \quad \mathbf{J} = \nabla \times \mathbf{B},$$

for a flat expanding universe with comoving and normalized $p = a^4 p_{\text{phys}}$, $\rho = a^4 \rho_{\text{phys}}$, $B_i = a^2 B_{i,\text{phys}}$, u_i , and conformal time t ($dt = a dt_c$).

¹³A. Brandenburg, et al., *Phys. Rev. D* **54**, 1291 (1996).

GW equation for a flat expanding Universe

- Assumptions: isotropic and homogeneous Universe.
- Friedmann–Lemaître–Robertson–Walker (FLRW) metric $\gamma_{ij} = a^2 \delta_{ij}$.
- Tensor-mode perturbations above the FLRW model:

$$g_{ij} = a^2 \left(\delta_{ij} + h_{ij}^{\text{phys}} \right), \quad |h_{ij}^{\text{phys}}| \ll |g_{ij}|$$

- GW equation is¹⁴

$$\left(\partial_t^2 - \frac{a''}{a} - c^2 \nabla^2 \right) h_{ij} = \frac{16\pi G}{a c^2} T_{ij}^{\text{TT}}$$

- h_{ij} are rescaled $h_{ij} = a h_{ij}^{\text{phys}}$.
- Comoving spatial coordinates $\nabla = a \nabla^{\text{phys}}$.
- Conformal time $dt = a dt_c$.
- Comoving stress-energy tensor components $T_{ij} = a^4 T_{ij}^{\text{phys}}$.
- Radiation-dominated epoch such that $a'' = 0$.

¹⁴L. P. Grishchuk, *Sov. Phys. JETP* **40**, 409 (1974).

Numerical results for decaying MHD turbulence¹⁵

Initial conditions

- Initial stochastic magnetic field with fractional helicity

$$\mathcal{P}_M = \frac{\mathcal{H}_M}{2\xi_M \mathcal{E}_M} = 2\sigma_M / (1 + \sigma_M^2)$$

- Batchelor spectrum, i.e., $E_M \propto k^4$ for small $k < k_* \sim \mathcal{O}(\xi_M^{-1})$.
- Kolmogorov spectrum in the inertial range, i.e., $E_M \propto k^{-5/3}$.

$$kB_i = \left(\delta_{ij} - \hat{k}_i \hat{k}_j - i\sigma_M \varepsilon_{ijl} \hat{k}_l \right) g_j \sqrt{2E_M(k)}$$

¹⁵ A. Brandenburg *et al.* (incl. ARP), *Phys. Rev. D* **96**, 123528 (2017).

ARP *et al.*, *Phys. Rev. D* **102**, 083512 (2020).

ARP *et al.*, *JCAP* **04** (2022), 019.

ARP *et al.*, *Phys. Rev. D* **105**, 123502 (2022).

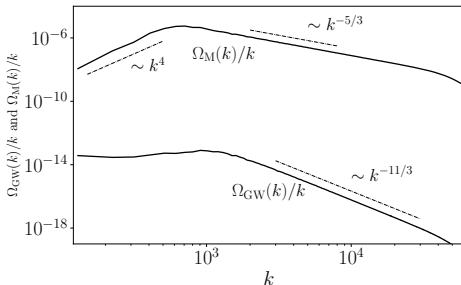
Numerical results for decaying MHD turbulence

Free parameters on the initial conditions

- Magnetic energy density at t_* is a fraction of the radiation energy density, $\Omega_M = \mathcal{E}_M / \mathcal{E}_{\text{rad}}^* = \frac{1}{2} B_0^2 \leq 0.1$ (BBN limit).
- Fractional helicity of the initial magnetic field via σ_M .
- Spectral peak k_* , normalized by H_*/c , is given by the characteristic scale of the sourcing turbulence (as a fraction of the Hubble radius) and should be $k_* \geq 2\pi$ by causality.
- Time t_* at which the magnetic field is generated, corresponding to the temperature scale T_* (e.g., $T_* \sim 100$ GeV at the electroweak phase transition).

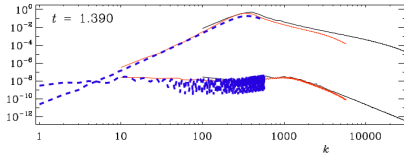
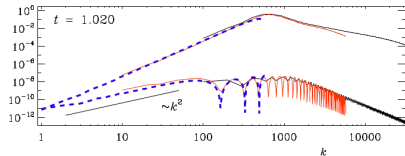
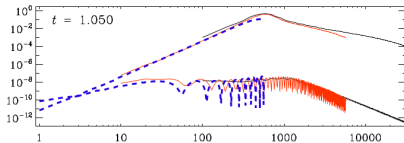
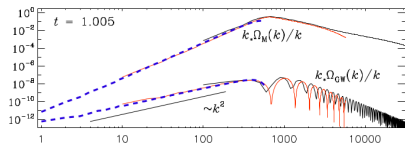
Numerical results for decaying MHD turbulence¹⁶

$$k_* = 2\pi \times 100, \Omega_M \sim 10^{-2}, \sigma_M = 1$$



- **Novel k^0 scaling in the subinertial range, i.e., $\Omega_{\text{GW}}(f) \sim f$.**
- k^2 is expected for larger scales, i.e., $\Omega_{\text{GW}}(f) \sim f^3$.

Early time evolution of the GW spectrum



Analytical model for decaying turbulence

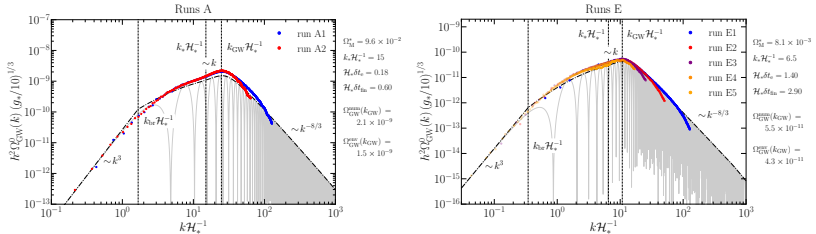
- Assumption: magnetic field evolution ($\delta t_e \sim 1/(v_A k_*)$) is slow compared to the GW dynamics ($\delta t_{\text{GW}} \sim 1/k$) at all $k \gtrsim v_A k_*$.
- We can derive an analytical expression for nonhelical fields of the envelope over the oscillations¹⁷ of $\Omega_{\text{GW}}(k)$.

$$\Omega_{\text{GW}}(k, t_{\text{fin}}) \approx 3 \left(\frac{k}{k_*} \right)^3 \Omega_{\text{M}}^*{}^2 \frac{\mathcal{C}(\alpha)}{\mathcal{A}^2(\alpha)} p_{\Pi} \left(\frac{k}{k_*} \right) \\ \times \begin{cases} \ln^2[1 + \mathcal{H}_* \delta t_{\text{fin}}] & \text{if } k \delta t_{\text{fin}} < 1, \\ \ln^2[1 + (k/\mathcal{H}_*)^{-1}] & \text{if } k \delta t_{\text{fin}} \geq 1. \end{cases}$$

- Improved models with specific turbulent decaying laws [with Caprini] and fractional helicity [with Caprini, Midiri] are under preparation for publication.

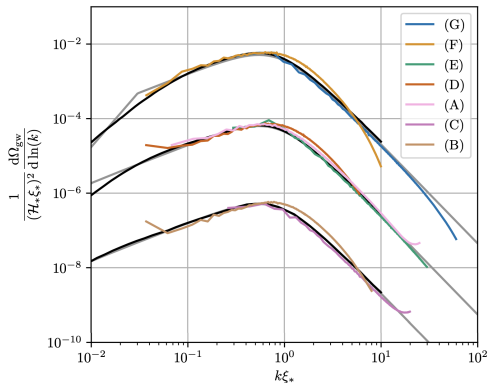
¹⁷ ARP et al., *Phys. Rev. D* **105**, 123502 (2022).

Numerical results for nonhelical decaying MHD turbulence¹⁸

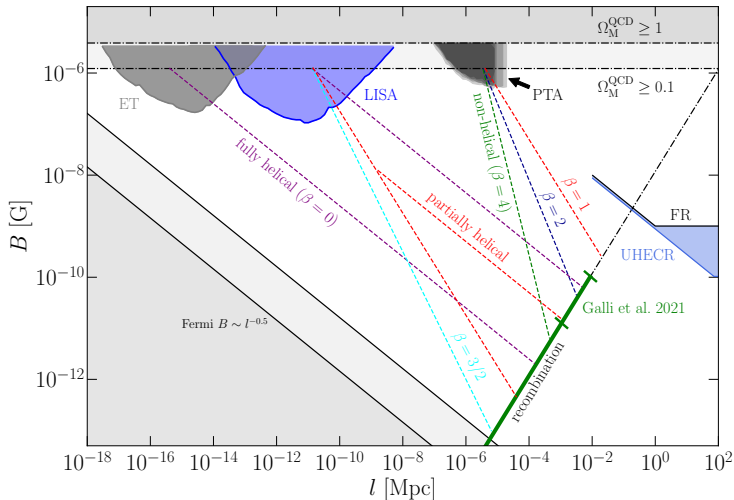


run	Ω_M^*	$k_* \mathcal{H}_*^{-1}$	$\mathcal{H}_* \delta t_e$	$\mathcal{H}_* \delta t_{fin}$	$\Omega_{GW}^{num}(k_{GW})$	$[\Omega_{GW}^{num}(k_{GW}) / \Omega_{GW}^{num}(k_{GW})]$	n	$\mathcal{H}_* L$	$\mathcal{H}_* t_{end}$	$\mathcal{H}_* \eta$
A1	9.6×10^{-2}	15	0.176	0.60	2.1×10^{-9}	1.357	768	6π	9	10^{-7}
A2	—	—	—	—	—	—	768	12π	9	10^{-6}
E1	8.1×10^{-3}	6.5	1.398	2.90	5.5×10^{-11}	1.184	512	4π	8	10^{-7}
E2	—	—	—	—	—	—	512	10π	18	10^{-7}
E3	—	—	—	—	—	—	512	20π	61	10^{-7}
E4	—	—	—	—	—	—	512	30π	114	10^{-7}
E5	—	—	—	—	—	—	512	60π	234	10^{-7}

Numerical results for nonhelical decaying HD vortical turbulence¹⁹



Using PTA,²⁰ LISA, and ET to constrain primordial magnetic fields
[unpublished]



²⁰ ARP et al., *Phys. Rev. D* **105**, 123502 (2022).

Numerical results for forced MHD turbulence²¹

Driven magnetic field

- Initial magnetic and velocity fields are zero.
- The magnetic field is forced during a short duration ($\sim 0.1 H_*^{-1}$) via the induction equation:

$$\frac{\partial \mathbf{B}}{\partial t} = \nabla \times (\mathbf{u} \times \mathbf{B} - \eta \mathbf{J} + \mathcal{F}).$$

- The forcing term is quasi-monochromatic with fractional magnetic helicity σ .

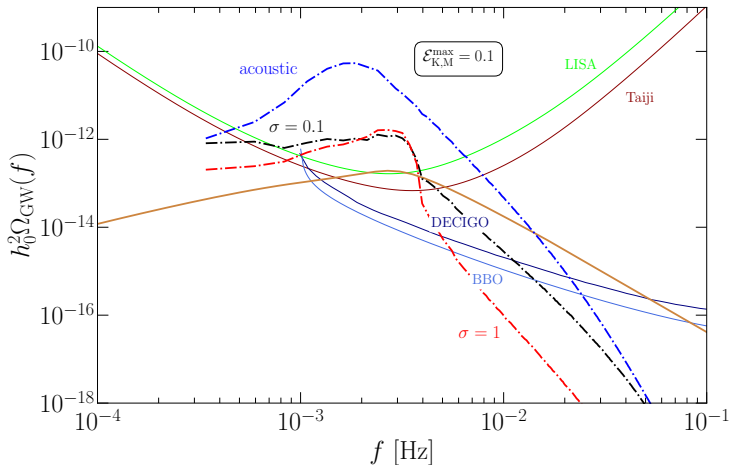
$$\mathcal{F} = \text{Re}(\mathcal{A}\mathbf{f}) \exp[i\mathbf{k} \cdot \mathbf{x} + i\phi], \quad k_* - \frac{1}{2}\delta k \leq |\mathbf{k}| \leq k_* + \frac{1}{2}\delta k,$$

$$f_i = \left(\delta_{ij} - i\sigma \varepsilon_{ijl} \hat{k}_l \right) f_j^{(0)} / \sqrt{1 + \sigma^2}.$$

²¹ ARP *et al.*, *Phys. Rev. D* **102**, 083512 (2020).

ARP *et al.*, *JCAP* **04** (2022), 019.

Using LISA to detect primordial magnetic fields at the
EWPT scale (forcing MHD turbulence)²²

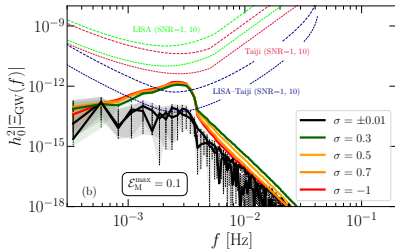
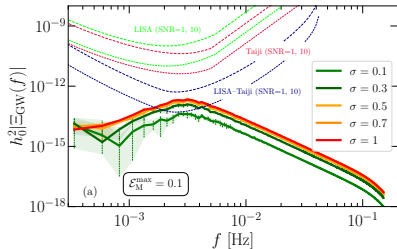


²² ARP *et al.*, *Phys. Rev. D* **102**, 083512 (2020).
 ARP *et al.*, *JCAP* **04** (2022), 019.
 ARP *et al.*, *Phys. Rev. D* **105**, 123502 (2022).

Using LISA and Taiji to detect the GW polarization²⁵

- LISA's dipole response function can provide us with a polarized gravitational wave background due to our proper motion.²³
- Cross-correlation of LISA and an additional space-based GW detector can improve the detectability of a polarized GW background.²⁴

$$\mathcal{P}_{\text{GW}}(k) = \frac{\Xi_{\text{GW}}(k)}{\Omega_{\text{GW}}(k)} = \frac{\langle \dot{\tilde{h}}_{\times} \dot{\tilde{h}}_{+}^{*} - \dot{\tilde{h}}_{+} \dot{\tilde{h}}_{\times}^{*} \rangle}{\langle \dot{\tilde{h}}_{+} \dot{\tilde{h}}_{+}^{*} + \dot{\tilde{h}}_{\times} \dot{\tilde{h}}_{\times}^{*} \rangle}$$



²³V. Domcke *et al.*, *JCAP* **05** (2020), 028.

²⁴G. Orlando, M. Pieroni and A. Ricciardone, *JCAP* **03** (2021), 069.

²⁵ARP *et al.*, *JCAP* **04** (2022), 019.

Conclusions 1/2

- Sources of MHD turbulence in the early universe can contribute to the stochastic GW background (SGWB).
- To study MHD turbulence we need, in general, to perform high-resolution numerical simulations.
- Since the SGWB is a superposition of different sources, it is extremely important to characterize the different sources, to be able to extract clean information from the early universe physics.
- The interplay between sound waves and the development of turbulence is not well understood. It plays an important role on the relative amplitude of both sources of GWs.
- We have performed simulations of MHD turbulence to study the SGWB produced by primordial magnetic fields and turbulence during cosmological phase transitions: at the QCD and at the electroweak scales.
- Pulsar Timing Arrays and space-based interferometers (LISA) can be used to probe the signals produced at cosmological phase transitions and, in particular, to constrain the characteristics of primordial magnetic fields.

Conclusions 2/2

- Magnetogenesis dynamics play a key role in the final GW spectral shape, even in the amplitude and peak, so we need to couple the early dynamics with our MHD simulations. **This is the objective of my current project with C. Caprini, A. Midiri and other collaborators, please contact me if you are interested!**
- Bubble nucleation and sound wave production can be coupled to our equations for more realistic production analysis.
- Production of helical magnetic fields can be related to Chern-Simons violations and to production of particles, shedding light on the baryon-asymmetry problem.
- The circular polarization of GWs produced by helical magnetic fields might not be detectable by LISA but it will be detectable by correlating LISA and one additional space-based GW detectors (e.g., Taiji)
- Probe of the origin of magnetic fields in the largest scales of our Universe, which is still an open question in cosmology.



The End Thank You!



alberto.roperpol@unige.ch

github.com/AlbertoRoper/GW_turbulence
cosmology.unige.ch/users/alberto-roper-pol